ARTICLE

Phase Transition and Oxygen Ion Diffusion in $(La_{1-x}Ln_x)_2Mo_2O_9$ (Ln=Nd, Gd, x=0.05-0.25) Using Dielectric Relaxation Method

Qian-feng Fang[a,b*], Zhong Zhuang[b], Xian-ping Wang[a,b], Dan Li[b], Jian-xin Wang[a]

a. Ningbo Institute of Material Technology and Engineering, Chinese Academy of Sciences, Ningbo 315040, China

b. Key Laboratory of Materials Physics, Institute of Solid State Physics, Chinese Academy of Sciences, Hefei 230031, China

(Dated: Received on September 16, 2007; Accepted on March 12, 2008)

Dielectric relaxation method was employed to study the properties of oxygen ion diffusion and phase transition in the oxide-ion conductors $(La_{1-x}Ln_x)_2Mo_2O_9$ (Ln=Nd, Gd, x=0.05-0.25). Two dielectric loss peaks were observed: peak P_d at about 600 K and peak P_h around 720 K. Peak P_d is a relaxational peak and associated with the short-range diffusion of oxygen ions, while peak P_h hardly changes its position and dramatically decreases in height with increasing frequency, exhibiting non-relaxational nature. With increasing Ln^{3+} concentration, the heights of peak P_h and P_d increase at first and then decrease after passing a maximum at 15% doping. It is suggested that peak P_h is related to the phase transition of a static disordered state to a dynamic disordered state in oxygen ions/vacancies distribution. It is found that the 15%Gd or 15%Nd doped $La_2Mo_2O_9$ samples exhibit the highest conductivity in accordance with the highest height of peak P_d at this doping content.

Key words: Oxide-ion conductor, $La_2Mo_2O_9$, Dielectric relaxation, Oxygen ion diffusion

I. INTRODUCTION

Oxide-ion conductors are promising materials that are widely used in solid oxide fuel cells, oxygen pumps, oxygen sensors, and other solid ionic devices [1-6]. As a novel oxide-ion conductor, lanthanum molybdate ($La_2Mo_2O_9$) has been attracting extensive attention in recent years since it was reported by Lacorre *et al.* in 2000 [7], owing to its novel structural type based on the lone pair substitution (LPS) concept [8], and outstanding ionic conduction properties at intermediate temperatures (873-1073 K) [9-12]. The high temperature β phase of $La_2Mo_2O_9$, a cubic structure with space group $P2_13$, exhibits ionic conductivity as high as 0.06 S/cm at 1073 K that is comparable to the conductivity of widely used yttria stabilized zirconia (YSZ) at 1273 K. However, a structural phase transition around 853 K, from the β phase to low-temperature monoclinic α phase, leads to a drop in conductivity by nearly two orders of magnitude [7-10]. Moreover, the change of crystal lattice constant induced by this phase transition would limit the mechanical stability and its potential practical application. In order to improve the conductivity and mechanical stability of $La_2Mo_2O_9$, various substitutions have been carried out at the La^{3+} sites or at Mo^{6+} sites to suppress this phase transition and maintain the high-conduction phase to lower temperatures. In the past several years, a series of compounds derived from pure $La_2Mo_2O_9$ have been investigated, in which La^{3+} has been replaced by Ca^{2+}, K^+, Sr^{2+}, Ba^{2+}, Bi^{3+}, Ln^{3+} (rare earth element), and Mo^{6+} by Nb^{5+}, Ta^{5+}, Re^{6+}, V^{5+}, S^{6+}, Cr^{6+}, and W^{6+} [10-31]. It is reported that $La_2Mo_2O_9$ samples doped at La site with lanthanide rare-earth ions such as Y^{3+}, Ce^{3+}, Nd^{3+}, Sm^{3+}, Eu^{3+}, Gd^{3+}, Dy^{3+}, and Er^{3+} have higher ionic conductivity than the pure $La_2Mo_2O_9$ sample [13,14,21-23,25]. When the doping content of some rare earth ions is above a certain value, β phase will be stabilized in the compound except for Nd^{3+} doping [13,14,23]. It is interesting to further study the rare earth ion doping because it does not change the concentration of total oxygen vacancies while resulting in a variation of lattice constant and the order (disorder) distribution of cations at La sites.

In previous studies, relaxational internal friction peaks and dielectric loss peaks associated with oxygen-ion diffusion were observed and a corresponding atomistic mechanism is suggested based on the crystalline structure of $La_2Mo_2O_9$ [10,15-19,26-29]. Recently, a non-relaxational internal friction peak associated with a phase transition from low-temperature static disordered state to high-temperature dynamic disordered state in distribution of oxygen ions/vacancies was observed in $La_2Mo_{2-x}W_xO_9$ [18], $La_{2-x}Ba_xMo_2O_{9-\delta}$ [24], and $La_{1.95}K_{0.05}Mo_{2-x}T_xO_{9-\delta}$ (T=Fe, Mn) [30]. Correspondingly, a dielectric loss peak was detected in $La_2Mo_{2-x}W_xO_9$ [31]. It is worthwhile to investigate whether such a peak appears in rare-earth ion doped $La_2Mo_2O_9$ compounds and how such a peak behaves. In the current research, the effects of Nd^{3+} and Gd^{3+} doping on the diffusion properties of oxygen ions and phase transition in oxide-ion conductor $La_2Mo_2O_9$ were

*Author to whom correspondence should be addressed. E-mail: qffang@issp.ac.cn, Tel: +86-551-5591459, fax: +86-551-5591434

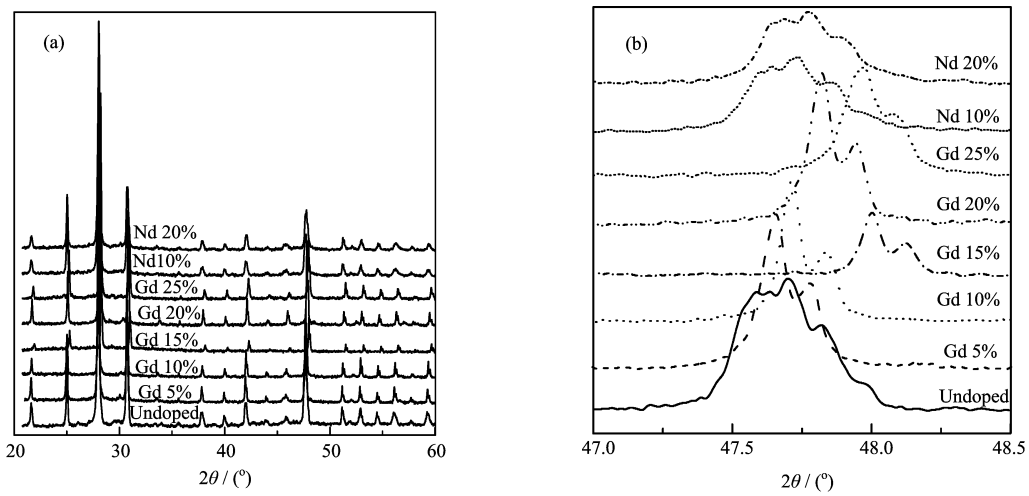

FIG. 1 (a) The XRD patterns of $(La_{1-x}Gd_x)_2Mo_2O_9$ (x=0.05-0.25), $La_2Mo_2O_9$, and $(La_{0.8}Nd_{0.2})_2Mo_2O_9$ samples. (b) The enlargement of the diffraction patterns of (321) reflection.

systematically investigated by dielectric relaxation technique.

II. EXPERIMENTS

All the compounds $(La_{1-x}Ln_x)_2Mo_2O_9$ (Ln=Nd, Gd, x=0.05-0.25) were prepared by conventional solid state reaction method. After the stoichiometric starting raw materials of high purity La_2O_3, Gd_2O_3, Nd_2O_3, and MoO_3 powders were well mixed in an agate mortar, the initial mixture powders were heated at 823 K for 12 h in an alumina crucible for pre-reaction to avoid MoO_3 sublimation, and then heated at 1223-1273 K for 12 h with two or three times intermediate grinding. At last, the powders were uniaxially pressed in a mold to form pellet samples (about 7 mm in diameter and 1 mm in thickness) and sintered at 1273-1293 K for 12 h. The relative density of all samples was about 90%-94%.

The powder X-ray diffraction (XRD) data were collected at room temperature with Cu-Kα radiation and a 2θ scan range from 20° to 80° with a scan step of 0.0167° on a Bragg-Brentano X'Pert MPD PRO diffractometer. The whole pattern matching refinement of XRD patterns was analyzed using the Fullprof Prog. The silver paste was pasted on both sides of the pellets and heated at 923 K for 30 min to form Ag electrodes with a thickness of about 0.1 mm for the dielectric measurements. The electrical connections to the experimental setup were achieved through platinum wires. The dielectric spectra of $(La_{1-x}Ln_x)_2Mo_2O_9$ (Ln=Nd, Gd, x=0.05-0.25) samples were measured using a HIOKI 3531 Z HITESTER. This setup operates in a frequency range from 50 Hz to 5 MHz, and the measurable values of the dielectric loss range from 10^{-5} to 10.

III. RESULTS AND DISCUSSION

The powder XRD of $(La_{1-x}Ln_x)_2Mo_2O_9$ samples with different substitution concentration are presented in Fig.1. At first glance, the patterns of all samples are similar, but after careful analysis there are differences in the details of the pattern. As shown in the Fig.1(b), the pure $La_2Mo_2O_9$ samples exhibit at least four peaks at 2θ around 47.7°, which are the splitting of Kα_1 and Kα_2 components of the 123 reflection owing to the monoclinic distortion in α phase. In all the Nd^{3+} doped samples, four peaks appear at 2θ around 47.7°, indicating the existence of α phase even at doping content as high as 20%Nd, while in the Gd^{3+} doped samples only two peaks are detected, indicating that more than 5%Gd doping can suppress the phase transition and stabilize the β phase to room temperature. This is in accordance with the previous results [7,9,13].

The lattice constants were computed from the refinements of XRD patterns as 0.7151 nm for $La_2Mo_2O_9$, 0.7127 nm for $La_{0.8}Gd_{0.2}Mo_2O_9$, and 0.7138 nm for $La_{0.8}Nd_{0.2}Mo_2O_9$ samples. The decrease in lattice constant illustrates that Ga or Nd ions were introduced into the lattice since the ionic radius of Nd^{3+} (1.163 Å) and Gd^{3+} (1.107 Å) is smaller than that of La^{3+} (1.216 Å) [13].

In order to find the influence of Nd or Gd substitution at La sites in $La_2Mo_2O_9$ on the oxygen-ion diffusion and phase transition, the dielectric relaxation properties of different doping concentrations was studied. The temperature dependence of dielectric loss (tanδ) at 1 kHz for $(La_{1-x}Gd_x)_2Mo_2O_9$ (x=0.05-0.25) and $(La_{0.8}Nd_{0.2})_2Mo_2O_9$ samples is shown in Fig.2. In all the investigated samples, two dielectric loss peaks, labeled as P_d and P_h, are observed. With increasing Gd concentration, peak P_d obviously shifts first toward higher temperature and then toward lower temperature, while for the peak P_h that is located around 720 K, the peak position is almost independent of the ratio of Gd/La. Except for peaks P_d and P_h, an obvious stepwise variation around 850 K is observed in the tanδ-T

DOI:10.1088/1674-0068/21/03/270-274

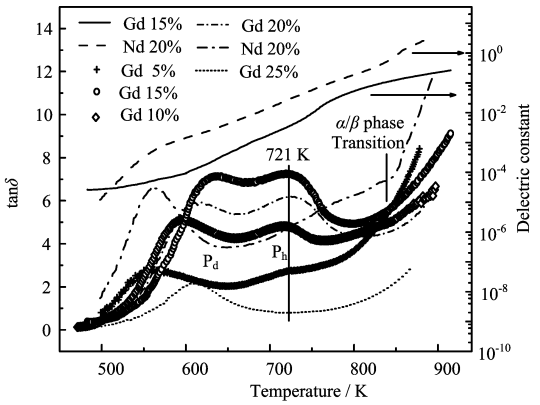

FIG. 2 The dielectric loss and dielectric constant as a function of temperature for $(La_{1-x}Gd_x)_2Mo_2O_9$ (x=0.05-0.25) and $(La_{0.8}Nd_{0.2})_2Mo_2O_9$ samples at the frequency of 1 kHz.

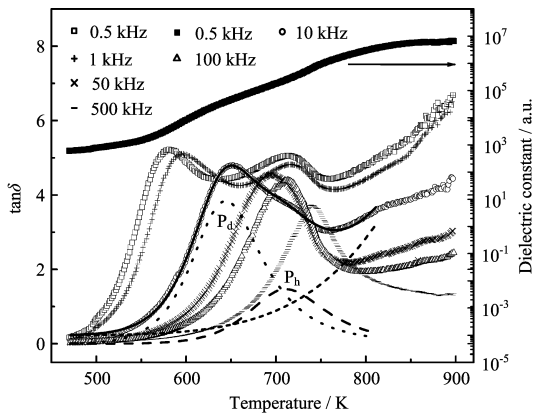

FIG. 3 Dielectric loss as a function of temperature for a $(La_{0.9}Gd_{0.1})_2Mo_2O_9$ sample at six different frequencies and the dielectric constant curve at 500 Hz. The decomposition of the data at 10 kHz into peak P_d (dot line), peak P_h (dash line), and background (short dash line), and the total fitting result (solid line) are also shown.

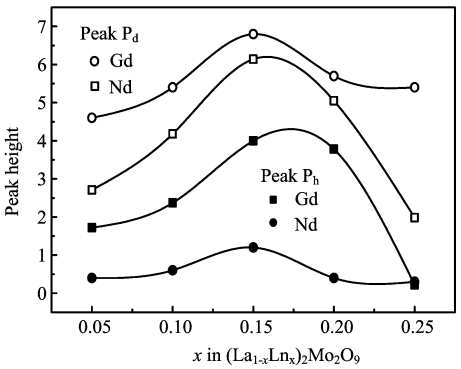

FIG. 4 Variation of peak height of P_d and P_h at a frequency of 1 kHz as a function of the doping content for $(La_{1-x}Gd_x)_2Mo_2O_9$ (x=0.05-0.25) and $(La_{1-x}Nd_x)_2Mo_2O_9$ (x=0.05-0.25) samples.

curves of the $(La_{0.8}Nd_{0.2})_2Mo_2O_9$ sample, as shown in Fig.2. This stepwise variation of dielectric loss with temperature is actually associated with the α/β phase transition, which is consistent with the results of XRD. In Gd-doped samples however, the dielectric loss curve changes smoothly in the range of the phase-transition temperature owing to the suppression of the α/β transition.

To further understand the characteristic of peaks P_d and P_h, dielectric loss curves at different frequencies were illustrated. As a typical example, Figure 3 illustrates the variation of dielectric loss and relative dielectric constant versus temperature for a 10%Gd doped sample at 0.5, 1, 10, 50, 100, and 500 kHz, where the curves were well fitted by two Debye peaks. It can be seen that with increasing frequency peak P_d shifts towards higher temperature and decreases a little in height, exhibiting typical relaxational nature. Meanwhile the relative dielectric constant changes dramatically around the peak positions.

It is well known that for a relaxational process the dielectric loss is a function of frequency f and temperature T and a peak would appear at $\omega\tau$=1, where ω=2πf is the angular frequency and τ is the relaxation time. As the frequency increases, the peak temperature T_p will increase according to the Arrhenius relation $\tau=\tau_0\exp(E/kT)$, where τ_0 is the pre-exponential factor of relaxation time, E is the activation energy of the relaxation process, and k is the Boltzmann constant. The activation energy and the pre-exponential factor of relaxation time of the P_d peak are deduced as 1.1 eV to 1.4 eV and 10^{-16} s to 10^{-14} s, respectively, depending upon the doping contents. These results imply that peak P_d is related to the short-distance jumps of oxygen ions via vacancies, analogous to the reported relaxation peak in other undoped or doped $La_2Mo_2O_9$ members [10,15-19,26-29].

The doping content dependence of the peak height of peak P_d is plotted in Fig.4 for both Gd^{3+} and Nd^{3+} doped samples. It can be seen from Fig.4 that with increasing doping content, peak P_d increases in height at first and then decreases after passing a maximum. At a comparable doping content, peak P_d in the Gd doped sample is lower than that in the Nd doped sample, in agreement with the effect of other doping elements that suppress the α/β phase transition [27,28]. It is interesting to note that a maximum of peak height appears around 15% doping content, which implies that the highest ionic conductivity at low temperatures may be exhibited in 15%Gd or 15%Nd doped samples because the peak height of P_d is proportional to the content of movable oxygen vacancies. This prediction is confirmed by the conductivity measurement.

However, as shown in Fig.3, peak P_h located around 720 K hardly changes its position but decreases in height rapidly with increasing frequency. Therefore peak P_h can be ascribed to a phase transition from low-temperature static disordered state to high-

DOI:10.1088/1674-0068/21/03/270-274

temperature dynamic disordered state in distribution of oxygen ions/vacancies, analogous to the reported results in other undoped or doped $La_2Mo_2O_9$ members [18,24,30,31].

In the oxygen sublattice of cubic $La_2Mo_2O_9$ compounds, the high atomic displacement parameters deduced from X-ray and neutron diffraction measurements suggest that the oxygen ions are delocalized, especially at the oxygen sites of O(2) and O(3) [9,13]. The extent of delocalization will increase with increasing temperature, and at a given temperature a random distribution of oxygen ions is formed when the zones of delocalization of two neighboring oxygen ions overlap with each other. This is the so-called dynamic disordered state in the oxygen sublattice where the oxygen ions and the vacancies can exchange their position easily and rapidly owing to the thermally assisting mechanism as suggested in Ref.[32]. With decreasing temperature, the dynamic disordered state will be frozen, becoming a static disordered state where the thermally assisted exchanging rate between oxygen ions and vacancies is very low. Therefore at a given temperature the phase transition from the static disordered state to the dynamic disordered state of oxygen ion/vacancy distribution occurred, which is similar to the glass transition process in amorphous compounds and polymers as well as to the formation process of spin glass in ferromagnetic materials.

The doping content dependence of the peak height of peak P_h is plotted in Fig.4 for both Gd^{3+} and Nd^{3+} doped samples. It can be seen that with increasing doping content, peak P_h increases in height at first and then decreases after passing a maximum. At a comparable doping content, peak P_h in the Gd doped sample is much higher than that in the Nd doped sample. Keeping in mind that the crystal structure is cubic β phase in the Gd doped sample while it is monoclinic α phase in the Nd doped samples, it can be concluded that peak P_h is only pronounced in doped $La_2Mo_2O_9$ samples in which the β phase is stabilized down to the room temperature. This is reasonable because only in the β phase is the distribution of oxygen ions/vacancies disordered, while in α phase it is mainly ordered. However, the fact that peak P_h with low intensity appears in Nd doped α-$La_2Mo_2O_9$ illustrates the existence of a small amount of disordered states in α-$La_2Mo_2O_9$, as pointed out in Ref.[33], which also undergoes the transition from the dynamic disordered state to the static disordered state. The variance of peak height of P_h with doping content of Gd and Nd illustrates that the transition from the static disordered state to the dynamic disordered state of oxygen ion/vacancy distribution depends upon the disordered degrees at cation sites (for example, La sites).

To simulate the complex AC impedance spectra, the bulk resistance, grain boundary resistance and electrode interface resistance were fitted by a serial circuit of three parallel RC equivalent circuits in the frequency range

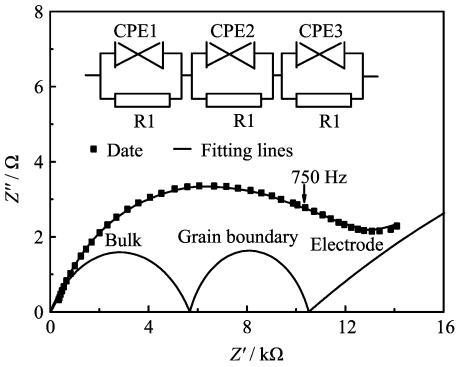

FIG. 5 Complex AC impedance spectra at 793 K for a $La_{0.9}Gd_{0.1}Mo_2O_9$ sample. The serial circuit of three parallel RC equivalent circuits in the frequency range simulated the bulk resistance, grain boundary resistance and electrode interface resistance.

analyzed, where R represents the bulk resistance and C the bulk or geometric capacitance of the samples. The bulk or geometric capacitance C is always replaced by CPE (constant phase angle element), when the curve of complex impedance data plotted in complex plane is not an ideal semicircle. As an example, Figure 5 presents the complex AC impedance spectra at 793 K and its serial equivalent circuit for a 5%Gd doped sample, where the semicircle at high frequency is composed of bulk resistance and grain boundary resistance. Based on this method, crystal grain resistance and intergranular resistance were computed, and the sum of the two resistances was used as total resistance of the sample, Rt. The electric resistivity, ρ, is deduced by the rule Rt=$\rho L/S$, where L is the length of the sample and the S is the area of the sample. The conductivity, σ=$1/\rho$, is presented in Fig.6 for $(La_{1-x}Gd_x)_2Mo_2O_9$ samples as an example. At a comparable temperature, the conductivity increases at first and then decreases with the increasing Gd doping concentration. The highest conductivity was obtained in the 15%Gd doped sample, where the highest P_d peak is observed as mentioned above. The co-appearance of the highest dielectric relaxation peak and the highest ionic conductivity in the doped $La_2Mo_2O_9$ samples is not just coincidental but has a physical meaning. This indicates that the 15%Gd doped sample has the highest concentration of the movable oxygen vacancies, because the height of the dielectric relaxation peak is proportional to the concentration of movable oxygen vacancies and the ionic conductivity is proportional to the products of this concentration with the mobility of vacancies. Dielectric relaxation peak and ionic conduction are realized by the short-range diffusion and long-distance migration of oxygen vacancies, respectively. They are so correlated that the long-distance migration of oxygen vacancies consists of a series of short-range diffusions. In this sense, a high relaxation peak associated with oxygen vacancies is consistent with high oxygen-ion conductivity.

DOI:10.1088/1674-0068/21/03/270-274

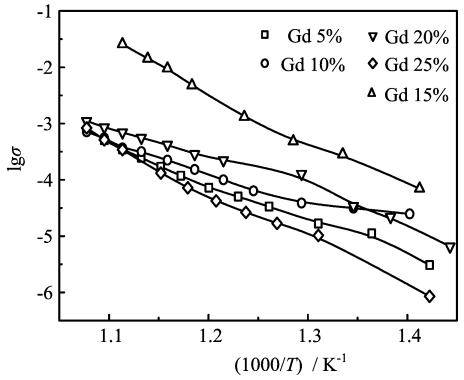

FIG. 6 Variation of conductivity with the reciprocal of temperature for $(La_{1-x}Gd_x)_2Mo_2O_9$ samples.

IV. CONCLUSION

Two dielectric loss peaks (P_d peak at lower temperature and P_h peak at higher temperature) were observed in Nd and Gd doped $La_2Mo_2O_9$ samples. Peak P_d is of relaxation type and related to the short-distance jumps of oxygen vacancies, while peak P_h is associated with a phase transition from the static disordered state to the dynamic disordered state of oxygen ion/vacancy distribution. Especially in Nd-doped $La_2Mo_2O_9$, the appearance of small peak P_h indicates the existence of a small number of disordered states in α-$La_2Mo_2O_9$, which also undergoes a transition from the dynamic disordered state to the static disordered state. With increasing Gd or Nd concentration, the heights of both peaks (P_h and P_d) increase at first and then decrease after passing a maximum at 15% doping content. Correspondingly, the conductivity of Gd doped samples increases at first and then decreases after passing a maximum at 15% doping content.

V. ACKNOWLEDGMENTS

This work was supported by the Ningbo Civic Natural Science Foundation (No.2006A610057), the Ningbo Civic Project of International Cooperation (No.2006B100080), Zhejiang Provincial Project of International Cooperation (No.2007C24022), and the National Natural Science Foundation of China (No.50672100 and No.50702061).

[1] H. Yahiro, T. Ohuchi, and K. Eguchi, J. Mater. Sci. **23**, 1036 (1988).
[2] A. Pimenov, J. Ullrich, P. Lunkenheimer, A. Loial, and C. H. Rscher, Solid State Ionics **109**, 111 (1988).
[3] N. Q. Minh, J. Am. Ceram. Soc. **76**, 563 (1993).
[4] K. R. Kendall, C. Navas, J. K. Thomas, and H. C. Z. Loye, Solid State Ionics **82**, 215 (1995).
[5] J. A. Lane, S. J. Benson, D. Waller, and J. A. Kilner, Solid State Ionics **121**, 201 (1999).
[6] J. A. Kilner, Solid State Ionics **13**, 129 (2000).
[7] P. Lacorre, F. Goutenoire, O. Bohnke, and R. Retoux, Nature **404**, 856 (2000).
[8] P. Lacorre, Solid State Sciences **2**, 755 (2000).
[9] F. Goutenoire, O. Isnard, and P. Lacorre, Chem. Mater. **12**, 2575 (2000).
[10] X. P. Wang and Q. F. Fang, Phys. Rev. B **65**, 06304 (2002).
[11] Z. S. Khadasheva, N. U. Venskovskii, M. G. Safronenko, A. V. Mosunov, E. D. Politova, and S. Y. Stefanovich, Inorg. Mater. **38**, 1381 (2002).
[12] R. A. Rocha, and E. N. Muccillo, Chem. Mater. **15**, 4268 (2003).
[13] S. Georges, F. Goutenoire, F. Altorfer, D. Sheptyakov, F. Fauth, E. Suard, and P. Lacorre, Solid State Ionics **161**, 231 (2003).
[14] D. Tsui, M. Hsieh, J. Tseng, and H. Lee, J. Euro. Ceram. Soc. **25**, 481 (2005).
[15] X. P. Wang and Q. F. Fang, Solid State Ionics **146**, 185 (2002).
[16] X. P. Wang, Q. F. Fang, Z. S. Li, G. G. Zhang, and Z. G. Yi, Appl. Phys. Lett. **81**, 3434 (2002).
[17] Q. F. Fang, X. P. Wang, Z. J. Cheng, and G. G. Zhang, Frontiers Mater. Sci. China **1**, 7-15 (2007).
[18] X. P. Wang, D. Li, Q. F. Fang, Z. J. Cheng, G. Cobel, and P. Lacorre, Appl. Phys. Lett. **89**, 021904 (2006).
[19] X. P. Wang, Z. J. Cheng, and Q. F. Fang, Solid State Ionics **176**, 761 (2005).
[20] P. Lacorre, A. Selmi, G. Corbel, and B. Boulard, Inorgan. Chem. **45**, 627 (2006).
[21] D. Marrero-Lopez, J. Canales-Vazquez, W. Z. Zhou, J. T. S. Irvine, and P. J. Nunez, Solid State Chem. **179**, 278 (2006).
[22] D. H. Tsai, M. J. Hsieh, J. C. Tseng, and H. Y. Lee, J. Euro. Ceram. Soc. **25**, 481 (2005).
[23] D. Marrero-Lopez, P. Nunez, M. Abril, V. Lavin, U. R. Rodrigueq-Mendoza, and V. D. Rodrigueq, J. Noncrystal. Solids **345**, 377 (2004).
[24] F. J. Liang, X. P. Wang, Q. F. Fang, J. X. Wang, C. Li, D. Li, and Z. Zhuang, Phys. Rev. B **74**, 014112 (2006).
[25] S. Georges, F. Goutenoire, Y. Laligant, and P. J. Lacorre, Mater. Chem. **13**, 2317 (2003).
[26] X. P. Wang and Q. F. Fang, J. Phys: Condens. Matter. **13**, 1641 (2001).
[27] Q. F. Fang, F. J. Liang, X. P. Wang, G. G. Zhang, and Z. J. Cheng, Mater. Sci. Eng. A. **442**, 43 (2006).
[28] Q. F. Fang, X. P. Wang, Z. G. Yi, and Z. J. Cheng, Solid State Phenomenon **115**, 193 (2006).
[29] C. Li, X. P. Wang, J. X. Wang, D. Li, Z. Zhuang, and Q. F. Fang, Mater. Res. Bull. **42**, 1077 (2007).
[30] C. Li, Q. F. Fang, X. P. Wang, J. X. Wang, D. Li, and Z. Zhuang, J. Appl. Phys. **101**, 083508 (2007).
[31] D. Li, X. P. Wang, Q. F. Fang, J. X. Wang, C. Li, and Z. Zhuang, Phys. Stat. Sol. A **204**, 2270 (2007).
[32] C. Bohnke and J. L. Foruquet, Solid State Ionics **91**, 21 (1996).
[33] I. R. Evans, J. A. K. Howard, and J. S. O. Evans, Chem. Mater. **17**, 4074 (2005).

DOI:10.1088/1674-0068/21/03/270-274